

CrossMark  
click for updatesCite this: *RSC Adv.*, 2014, 4, 46378Received 11th May 2014  
Accepted 15th September 2014

DOI: 10.1039/c4ra04397a

www.rsc.org/advances

## An efficient noble metal-free Ce–Sm/SiO<sub>2</sub> nano-oxide catalyst for oxidation of benzylamines under ecofriendly conditions†

Putla Sudarsanam, A. Rangaswamy and Benjaram M. Reddy\*

A nanosized Ce–Sm/SiO<sub>2</sub> catalyst was found to show an outstanding performance in the oxidation of benzylamines into valuable dibenzylimine products with almost 100% selectivity with O<sub>2</sub> as the green oxidant under solvent-free conditions, which is attributed to the presence of abundant strong acidic sites, enhanced oxygen vacancy concentration, and superior BET surface area.

Selective oxidation reactions are the most fundamental functional group transformations in organic chemistry.<sup>1–4</sup> In particular, the selective oxidation of amines into imines is a topic of significant research investigation in recent years due to extensive use of imines in the chemical industry.<sup>5,6</sup> Imines are vital electrophilic reagents for a number of organic reactions, which include alkylation, condensation, reduction, cycloaddition, *etc.* Imines are also crucial intermediates for the synthesis of medicines and biologically active compounds.<sup>7</sup> Several oxidation procedures that make use of hazardous stoichiometric oxidants, such as 2-iodoxybenzoic acid and *N*-tert-butylphenylsulfonimidoyl chloride, along with Ru-, Ir-, and Cu-based homogeneous catalysts have been reported for amine oxidation.<sup>7–10</sup> Alternatively, numerous heterogeneous catalysts, especially based on precious metals (*e.g.*, Au, Ru, and Pd) have been developed for amine oxidation.<sup>7,10–15</sup> Although these methods are quite interesting, the combination of a promising noble metal-free heterogeneous catalyst with molecular O<sub>2</sub> as green oxidant is essential for amine oxidation from the viewpoints of both economical and environmental concerns.<sup>5,16,17</sup>

Development of ceria-based materials with favourable properties is of immense research interest to the scientific community during the past few years, not only due to their

commercial exploitation in auto-exhaust purification, but also due to their significant use for various organic transformations.<sup>18,19</sup>

One of the most notable features of ceria is that it easily forms ample oxygen vacancy defects by preserving its fluorite-structure when an appropriate metal ion (*e.g.*, Sm<sup>3+</sup>, Fe<sup>3+</sup>, *etc.*) is introduced into the ceria lattice.<sup>20–22</sup> Consequently, the structural and redox properties of ceria are greatly improved, resulting in remarkable catalytic performance. Moreover, owing to their unique and fascinating physicochemical properties, the ceria-based oxides can selectively activate organic molecules to yield the desirable products.<sup>18</sup> It was also shown that reducing the ceria particle size to nanoscale range leads to a decrease in oxygen vacancy formation energy and thereby, an improved catalytic activity towards oxidation reactions.<sup>20</sup> The dispersion of ceria-based mixed oxides on an inert support (*e.g.*, SiO<sub>2</sub>) is one of the efficient approaches to improve the CeO<sub>2</sub> properties further as well as to reduce its particle size.<sup>23,24</sup>

Motivated by the above observations, we developed a novel and promising ceria-based catalyst *i.e.*, Sm-doped CeO<sub>2</sub> dispersed on SiO<sub>2</sub> (Ce–Sm/SiO<sub>2</sub>) for the aerobic oxidation of various benzylamines under ecofriendly reaction conditions. The selection of Sm in the present work is mainly due to its resemblance in the ionic radius and electro negativity with respect to Ce.<sup>21</sup> The nano-structured Ce–Sm/SiO<sub>2</sub> catalyst showed an interesting performance in the aerobic oxidation of various benzylamines with ~100% selectivity to imine products. We employed a highly practicable synthesis procedure based on precipitation of metal nitrate precursors for the preparation of the investigated Ce–Sm/SiO<sub>2</sub> nano-oxides (ESI†). For comparison purpose, pure CeO<sub>2</sub> and Sm-doped CeO<sub>2</sub> samples were also prepared by adopting the same synthesis procedure. A linear correlation was found between the concentration of strong acidic sites, BET surface area, oxygen vacancy concentration, and the oxidation performance of the synthesized catalysts. A thorough multi-technique analysis detailing structural and electronic properties of the synthesized samples was also undertaken (ESI†).

*Inorganic and Physical Chemistry Division, CSIR–Indian Institute of Chemical Technology, Uppal Road, Hyderabad–500 007, India. E-mail: bmreddy@iict.res.in; mreddyb@yahoo.com; Fax: +91 40 2716 0921; Tel: +91 40 2719 3510*

† Electronic supplementary information (ESI) available: Details concerning the synthesis and characterization results of ceria-based materials; TEM, XPS, FTIR, time-on-stream and reusable analysis of the CeO<sub>2</sub>-based samples for benzylamine oxidation. See DOI: 10.1039/c4ra04397a

The XRD and Raman profiles of the investigated CeO<sub>2</sub>-based materials are shown in Fig. 1A and B, respectively. It was found that all samples exhibit the characteristic XRD patterns of fluorite-structured CeO<sub>2</sub>.<sup>25,26</sup> Raman spectra show a sharp peak at  $\sim 450\text{--}460\text{ cm}^{-1}$  for all samples, attributed to Raman-active F<sub>2g</sub> mode of fluorite-structured CeO<sub>2</sub>, in line with the XRD results.<sup>27</sup> Interestingly, no XRD and Raman peaks corresponding to Sm<sub>2</sub>O<sub>3</sub> were found, which confirm the doping of Sm cations into the CeO<sub>2</sub> lattice. It was obvious from Fig. 1A and B that the addition of dopant (Sm) and support (SiO<sub>2</sub>) strongly modifies the XRD patterns as well as Raman spectrum of pristine CeO<sub>2</sub>. The estimated lattice parameter, average crystallite size, and F<sub>2g</sub> peak position of the samples confirm the above observations (Table 1). Hence, the incorporation of Sm<sup>3+</sup> ions into the CeO<sub>2</sub> lattice could favourably modify its structural properties for the aerobic oxidation of benzylamines as discussed in the later paragraphs.

Two additional Raman bands are found for Ce–Sm and Ce–Sm/SiO<sub>2</sub> samples. The appearance of Raman band at  $\sim 560\text{ cm}^{-1}$  indicates the presence of oxygen vacancies in the ceria-based materials, whereas the band at  $\sim 606\text{ cm}^{-1}$  reveals the SmO<sub>8</sub> defect complex.<sup>21</sup> We estimated the concentration of oxygen vacancies from the ratio of oxygen vacancy band (O<sub>v</sub>) to F<sub>2g</sub> band (O<sub>v</sub>/F<sub>2g</sub>) in such a way that a higher ratio means a higher oxygen vacancy concentration. It is interesting to note that the Ce–Sm/SiO<sub>2</sub> sample shows higher oxygen vacancy concentration (O<sub>v</sub>/F<sub>2g</sub> = 0.1053) than that of the Ce–Sm sample (O<sub>v</sub>/F<sub>2g</sub> = 0.0948). Moreover, the Ce–Sm/SiO<sub>2</sub> catalyst exhibits superior BET surface area (188 m<sup>2</sup> g<sup>−1</sup>) compared with Ce–Sm (84 m<sup>2</sup> g<sup>−1</sup>) and pristine CeO<sub>2</sub> (41 m<sup>2</sup> g<sup>−1</sup>) samples (Table 1).

As can be noted from the Fig. 1C and D, the Ce–Sm/SiO<sub>2</sub> sample contains nearly spherical shaped particles and fall in

the nanoscale range ( $\sim 8\text{--}12\text{ nm}$ ). The selected area electron diffraction patterns of Ce–Sm/SiO<sub>2</sub> reveal cubic structured CeO<sub>2</sub> with (111), (200), (220), and (311) planes, supporting the observations made from the XRD studies (Fig. 1A). The Ce–Sm/SiO<sub>2</sub> sample is well crystalline and the shape of the most crystallites is compatible with an octahedron defined by (111) facet at 3.1 Å (Fig. 1D). TEM and HRTEM images of the Ce–Sm sample provide evidence of the formation of nanosized particles in the range of 10–15 nm (Fig. S1, ESI†).

To our surprise, the Ce 3d spectrum of Ce–Sm/SiO<sub>2</sub> sample is noticeably different from that of the Ce–Sm and CeO<sub>2</sub> samples (Fig. 2A). Very much low binding energy of u<sup>///</sup> peak ( $\sim 912.6\text{ eV}$ ) was found for the Ce–Sm/SiO<sub>2</sub> compared with Ce–Sm (916.9 eV) and CeO<sub>2</sub> (917.5 eV), which strongly indicates the facile reducible nature of the Ce–Sm/SiO<sub>2</sub> sample.<sup>22</sup> It is generally accepted that the reducible nature of CeO<sub>2</sub> (*i.e.*, Ce<sup>4+</sup> → Ce<sup>3+</sup>) highly depends on generation of oxygen vacancies.<sup>22,28</sup> Hence, there is a huge possibility for the formation of more number of oxygen vacancies in the Ce–Sm/SiO<sub>2</sub> compared with the Ce–Sm oxide, in line with Raman results (Fig. 1B). Two peaks were found in the O 1s XP spectra of the ceria-based samples (Fig. S2, ESI†).<sup>28,29</sup> The lower energy peak denotes the ceria lattice oxygen, which is considerably varied for the Ce–Sm/SiO<sub>2</sub> sample in comparison to Ce–Sm and CeO<sub>2</sub> samples. Appearance of another peak at higher binding energy side signifies adsorbed oxygen species of hydroxyl and carbonate groups on the catalyst surface, as confirmed by FT-IR study (Fig. S3, ESI†).

The Sm 3d<sub>5/2</sub> XP spectra of Ce–Sm and Ce–Sm/SiO<sub>2</sub> samples show a peak at higher binding energy side, which confirm the presence of Sm in the 3+ oxidation state (Fig. 2B).<sup>30</sup> Another peak was found at lower binding energy side due to the strong charge transfer effect of the unpaired 4f electrons in Sm<sub>2</sub>O<sub>3</sub>. Interestingly, the intensity of the charge transfer band is much higher for the Ce–Sm/SiO<sub>2</sub> compared with that of the Ce–Sm sample.<sup>30–32</sup> This unusual observation reveals that the number of unpaired 4f electrons increases by more than one during the creation of the 3d<sup>−1</sup> core hole in the Ce–Sm/SiO<sub>2</sub> sample, thus making it more positively charged. This result also explains the Sm 3d<sub>5/2</sub> peak shift of the Ce–Sm/SiO<sub>2</sub> sample towards higher binding energy side. It is therefore expected that these unusual electronic modifications of Ce, Sm and O could improve the acidic properties of the Ce–Sm/SiO<sub>2</sub> sample. To understand this, the acidic properties of Ce–Sm and Ce–Sm/SiO<sub>2</sub> samples were investigated by means of NH<sub>3</sub>-TPD analysis (Fig. 2C). The relative position of the peak maxima in Fig. 2C indicates the magnitude of NH<sub>3</sub> desorption activation energy, and therefore, the relative strength of the acidic sites.<sup>33</sup> As shown in Fig. 2C, the NH<sub>3</sub>-TPD peaks can be assigned to before and after 673 K, corresponding to low-temperature (LT) and high-temperature (HT) regions, respectively.<sup>34</sup> The HT peak reveals NH<sub>3</sub> desorption from the strong acidic sites, whereas the LT peaks are attributed to release of NH<sub>3</sub> from the weak acid sites. It was apparent from Fig. 2C that the Ce–Sm/SiO<sub>2</sub> sample contains both strong- and weak-acidic sites, whereas the Ce–Sm sample has only weak acidic sites. This could be the reason for the observed high catalytic efficiency of the Ce–Sm/SiO<sub>2</sub> sample in

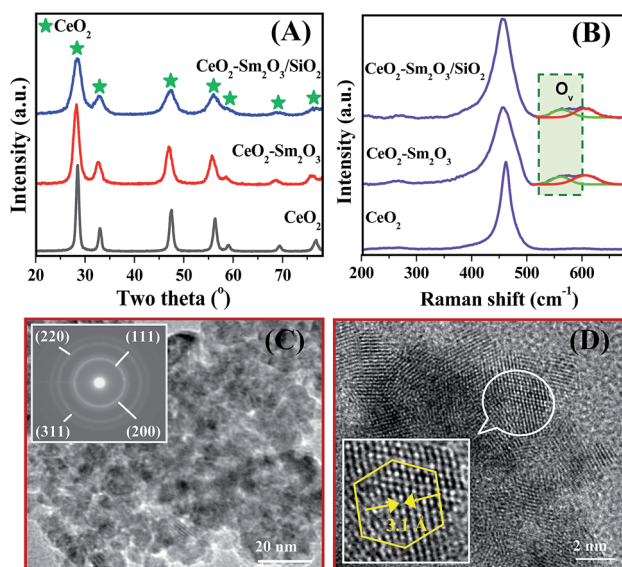
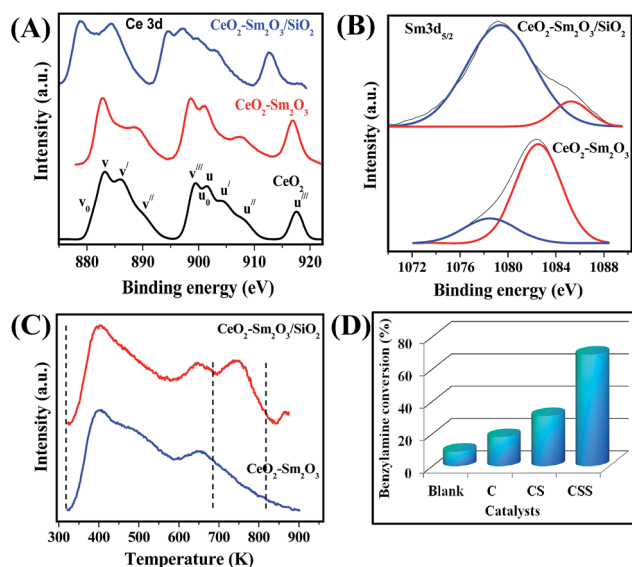


Fig. 1 (A) Powder XRD and (B) Raman profiles of CeO<sub>2</sub>-based materials (O<sub>v</sub>-oxygen vacancy band); (C) TEM image of Ce–Sm/SiO<sub>2</sub> and the corresponding selected-area electron diffraction (SAED) pattern; and (D) HRTEM image of Ce–Sm/SiO<sub>2</sub> (inset: enlarged view of selected area).

**Table 1** BET surface area (BET SA), average crystallite size ( $D$ ), lattice parameter (LP), and  $F_{2g}$  peak position of  $CeO_2$ -based catalysts. Standard deviations for BET SA and  $D$  values are  $\pm 5 \text{ m}^2 \text{ g}^{-1}$  and  $\pm 0.5 \text{ nm}$ , respectively

Sample	BET SA ( $\text{m}^2 \text{ g}^{-1}$ )	$D$ (nm) <sup>a</sup>	LP (nm) <sup>a</sup>	$F_{2g}$ peak position ( $\text{cm}^{-1}$ ) <sup>b</sup>
$CeO_2$	41	8.9	0.541	461
$CeO_2\text{-}Sm_2O_3$	84	7.6	0.545	456
$CeO_2\text{-}Sm_2O_3/SiO_2$	188	5.1	0.543	454

<sup>a</sup> From XRD studies. <sup>b</sup> From Raman spectra.



**Fig. 2** (A) Ce 3d and (B) Sm 3d<sub>5/2</sub> XPS spectra of  $CeO_2$ -based samples. (C)  $NH_3$ -TPD profiles of  $CeO_2\text{-}Sm_2O_3$  and  $CeO_2\text{-}Sm_2O_3/SiO_2$  samples, and (D) catalytic performance of  $CeO_2$  (C),  $CeO_2\text{-}Sm_2O_3$  (CS), and  $CeO_2\text{-}Sm_2O_3/SiO_2$  (CSS) samples for aerobic oxidation of benzylamine. Reaction conditions: benzylamine (0.2 mmol), catalyst amount (0.2 g),  $O_2$  bubbling rate ( $20 \text{ mL min}^{-1}$ ), reaction time (4 h), and temperature (393 K).

the aerobic oxidation of benzylamine as discussed in the later paragraphs.

Fig. 2D shows the catalytic performance of  $CeO_2$ ,  $Ce\text{-}Sm$ , and  $Ce\text{-}Sm/SiO_2$  samples for the oxidation of benzylamine using  $O_2$  as a green oxidant under solvent-free conditions. Very low benzylamine conversions were found for  $CeO_2$  (~16%) and  $Ce\text{-}Sm$  (~31%) samples compared with the  $Ce\text{-}Sm/SiO_2$  sample (~69%) for 4 h of reaction time. When the reaction time was increased to 6 h, almost 100% amine conversion was found for the  $Ce\text{-}Sm/SiO_2$  sample (Fig. S4, ESI†). In contrast, ~38 and 72% of amine conversions were achieved with the bare  $CeO_2$  and  $Ce\text{-}Sm$  samples for 6 h. However, it must be mentioned here that the activity of the  $Ce\text{-}Sm/SiO_2$  sample is very much low at initial reaction times (*i.e.*, ~12% amine conversion for 1 h of reaction time). A remarkable finding in the present investigation is that all samples exhibit superior selectivity of dibenzylimine product (~100%). Interestingly, when the reaction was conducted in the absence of catalyst (blank test), only 9% of amine conversion was observed. This result indicates the significance of ceria-based catalysts in the aerobic oxidation of

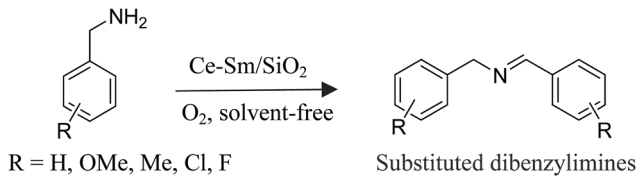
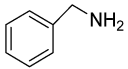
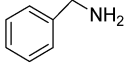
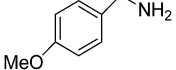
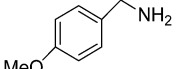
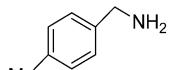
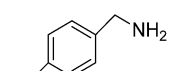
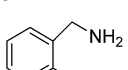
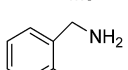
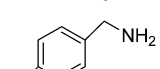
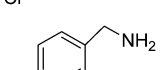
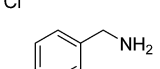
benzylamine. The presence of strong acidic sites, along with abundant oxygen vacancies and larger BET surface area are found to be the crucial factors for the observed enhanced activity of the  $Ce\text{-}Sm/SiO_2$  catalyst.

We investigated the scope of the  $Ce\text{-}Sm/SiO_2$  catalyst for the aerobic oxidation of various substituted benzylamines. As summarized in Table 2, substituted benzylamines can also be selectively oxidized into the corresponding imines using the  $Ce\text{-}Sm/SiO_2$  catalyst. Amongst, the highest amine conversion was achieved with *p*-MePhNH<sub>2</sub> (Table 2, entries 3 & 4) attributed to more basic nature of the amine and thereby, strong interaction between the amine and  $Ce\text{-}Sm/SiO_2$  catalyst, resulting in high amine conversion.<sup>11</sup> Very low amine conversion was found for 2-MePhNH<sub>2</sub> (Table 2, entries 7 & 8) compared with 4-MePhNH<sub>2</sub> (Table 2, entries 5 & 6), which might be due to steric hindrance of the methyl group at 2-position. Reasonable amine conversions were achieved in the case of halogen (Cl and F) substituted amines (Table 2, entries 9–11), which are highly useful synthons for the synthesis of chiral amines.<sup>35</sup>

We also studied the reusability of the  $Ce\text{-}Sm/SiO_2$  catalyst to understand its stability for the aerobic amine oxidation (Fig. S5, ESI†). The catalytic experiments were fixed as follows: benzylamine (0.2 mmol), catalyst amount (0.2 g),  $O_2$  bubbling rate ( $20 \text{ mL min}^{-1}$ ), reaction time (6 h), and temperature (393 K). After each run, the catalyst was washed with acetone to remove reaction gradients and then pre-activated at 423 K for 2 h. It was found that the  $Ce\text{-}Sm/SiO_2$  catalyst could be used repeatedly up to 4 cycles for amine oxidation without any significant loss of the activity, and ~100 and 90% benzylamine conversions were obtained for the 1<sup>st</sup> and 4<sup>th</sup> cycles, respectively. After 4<sup>th</sup> cycle, the performance of the  $Ce\text{-}Sm/SiO_2$  catalyst was considerably decreased. Approximately, 72 and 59% amine conversions were obtained for the 5<sup>th</sup> and 6<sup>th</sup> cycles, respectively. Understanding the reasons for the decrease in activity of the  $Ce\text{-}Sm/SiO_2$  catalyst after several recycling experiments are under further investigation. Despite the decrease in amine conversion with repeated use of the catalyst, no variation in the selectivity of the product was observed. On the whole, the  $Ce\text{-}Sm/SiO_2$  is a promising and recyclable noble-metal-free catalyst for aerobic oxidation of benzylamine under eco-friendly reaction conditions.

The aerobic oxidation of benzylamine into dibenzylimine usually follows two steps (Scheme 1).<sup>10,11</sup> First, an imine intermediate ( $PhCH=NH$ ) is formed through the oxidative dehydrogenation of benzylamine. Afterward, the unstable imine intermediate reacts instantly with benzylamine to form an

Table 2 Aerobic oxidation of various substituted benzylamines over the Ce–Sm/SiO<sub>2</sub> catalyst

<div style="text-align: center;">  <p>R = H, OMe, Me, Cl, F</p> <p>Substituted dibenzylimines</p> </div>				
Entry	Substrate	Time (h)	Amine conversion (%) <sup>a</sup>	Imine selectivity (%) <sup>b</sup>
1		4	69	99.9
2		6	~100	99.9
3		4	90	99.8
4		5	~100	99.6
5		4	53	99.9
6		6	91	99.7
7		4	45	99.9
8		6	85	99.7
9		4	65	99.8
10		6	96	99.6
11		6	93	99.7

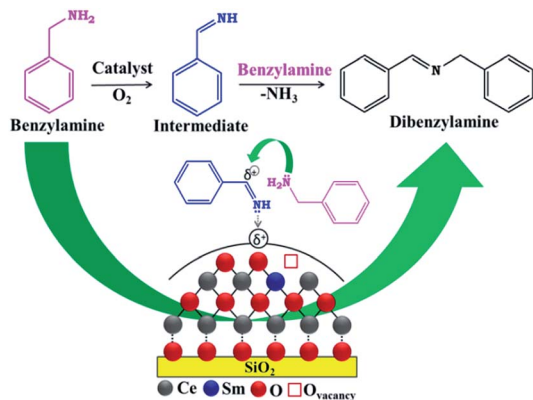
<sup>a</sup> Reaction conditions: substituted benzylamine (0.2 mmol), catalyst amount (0.2 g), O<sub>2</sub> bubbling rate (20 mL min<sup>−1</sup>), and temperature (393 K).<sup>b</sup> Very small amount of nitrile product was formed.

aminal followed by release of NH<sub>3</sub> to give the final dibenzylimine product. Alternatively, the dibenzylimine product can also be formed by the transformation of imine intermediate into benzaldehyde, which subsequently reacts with the available benzylamine to give dibenzylimine. It was obvious from Scheme 1 that the intermediate imine has net positivity charge, thus there is a high possibility for the attack of benzylamine on imine intermediate due to the presence of lone pair on the nitrogen atom of the benzylamine rather than the formation of benzaldehyde from imine intermediate. As stated, no benzaldehyde was found in the present study, confirming the

formation of imine product through the aminal formation followed by NH<sub>3</sub> release. It is a well-known fact in the literature that acid catalysts show remarkable efficiency in the amine oxidation through activation of C=N bond of imine intermediate.<sup>36–38</sup> Hence, the strong acidic nature of the Ce–Sm/SiO<sub>2</sub> catalyst is a key factor for its exceptional performance in the aerobic oxidation of benzylamines.

In conclusion, we have developed a novel nanostructured Ce–Sm/SiO<sub>2</sub> catalyst for efficient aerobic oxidation of various benzylamines under ecofriendly conditions. The Ce–Sm/SiO<sub>2</sub> catalyst showed almost 100% benzylamine conversion with





Scheme 1 Possible mechanism for the aerobic oxidation of benzylamine over the Ce-Sm/SiO<sub>2</sub> catalyst.

100% selectivity to dibenzylimine for 6 h of reaction time. This catalyst also selectively converts various substituted benzylamines into the corresponding imines with moderate to excellent yields. A remarkably finding observed in the present study is that the Ce-Sm/SiO<sub>2</sub> catalyst can be used repeatedly up to 4 times without any significant loss of the activity and selectivity. The strong acidic nature of the Ce-Sm/SiO<sub>2</sub> catalyst along with superior BET surface area and enhanced concentration of oxygen vacancies are crucial factors for its outstanding performance in the aerobic oxidation of benzylamines.

## Acknowledgements

P.S. and A.R. thank the Council of Scientific and Industrial Research (CSIR), New Delhi for research fellowships.

## References

- 1 X. F. Wu, C. B. Bheeter, H. Neumann, P. H. Dixneuf and M. Beller, *Chem. Commun.*, 2012, **48**, 12237–12239.
- 2 Z. Guo, B. Liu, Q. Zhang, W. Deng, Y. Wang and Y. Yang, *Chem. Soc. Rev.*, 2014, **43**, 3480–3524.
- 3 N. Dimitratos, J. A. Lopez-Sanchez and G. J. Hutchings, *Chem. Sci.*, 2012, **3**, 20–44.
- 4 M. Sankar, E. Nowicka, E. Carter, D. M. Murphy, D. W. Knight, D. Bethell and G. J. Hutchings, *Nat. Commun.*, 2014, **5**, 3332–3337.
- 5 S. Ahmad, K. Gopalaiah, S. N. Chandrudu and R. Nagarajan, *Inorg. Chem.*, 2014, **53**, 2030–2039.
- 6 L. Tang, H. Sun, Y. Li, Z. Zha and Z. Wang, *Green Chem.*, 2012, **14**, 3423–3428.
- 7 S. Furukawa, A. Suga and T. Komatsu, *Chem. Commun.*, 2014, **50**, 3277–3280.
- 8 L.-P. He, T. Chen, D. Gong, Z. Lai and K.-W. Huang, *Organometallics*, 2012, **31**, 5208–5211.
- 9 W. H. Bernskoetter and M. Brookhart, *Organometallics*, 2008, **27**, 2036–2045.
- 10 M. T. Schümperli, C. Hammond and I. Hermans, *ACS Catal.*, 2012, **2**, 1108–1117.
- 11 R. J. Angelici, *Catal. Sci. Technol.*, 2013, **3**, 279–296.
- 12 A. Grierrane, A. Corma and H. Garcia, *J. Catal.*, 2009, **264**, 138–144.
- 13 L. Aschwandten, T. Mallat, F. Krumeich and A. Baiker, *J. Mol. Catal. A: Chem.*, 2009, **309**, 57–62.
- 14 K. Yamaguchi and N. Mizuno, *Angew. Chem., Int. Ed.*, 2003, **42**, 1480–1483.
- 15 X. Jin, Y. Liu, Q. Lu, D. Yang, J. Sun, S. Qin, J. Zhang, J. Shen, C. Chu and R. Liu, *Org. Biomol. Chem.*, 2013, **11**, 3776–3780.
- 16 R. D. Patil and S. Adimurthy, *RSC Adv.*, 2012, **2**, 5119–5122.
- 17 R. D. Patil and S. Adimurthy, *Adv. Synth. Catal.*, 2011, **353**, 1695–1700.
- 18 L. Vivier and D. Duprez, *ChemSusChem*, 2010, **3**, 654–678.
- 19 C. Sun, J. Sun, G. Xiao, H. Zhang, X. Qiu, H. Li and L. Chen, *J. Phys. Chem. B*, 2006, **110**, 13445–13452.
- 20 S. M. Kozlova and K. M. Neyman, *Phys. Chem. Chem. Phys.*, 2014, **16**, 7823–7829.
- 21 K. Kuntaiah, P. Sudarsanam, B. M. Reddy and A. Vinu, *RSC Adv.*, 2013, **3**, 7953–7962.
- 22 P. Sudarsanam, B. Mallesham, D. N. Durgasri and B. M. Reddy, *RSC Adv.*, 2014, **4**, 11322–11330.
- 23 C. Sun, H. Lia and L. Chen, *Energy Environ. Sci.*, 2012, **5**, 8475–8505.
- 24 L. Katta, P. Sudarsanam, B. Mallesham and B. M. Reddy, *Catal. Sci. Technol.*, 2012, **2**, 995–1004.
- 25 P. Munusamy, S. Sanghavi, T. Varga and T. Suntharampillai, *RSC Adv.*, 2014, **4**, 8421–8430.
- 26 C. Sun and L. Chen, *Eur. J. Inorg. Chem.*, 2009, 3883–3887.
- 27 P. Bharali, P. Saikia and B. M. Reddy, *Catal. Sci. Technol.*, 2012, **2**, 931–933.
- 28 P. Sudarsanam, B. Mallesham, P. S. Reddy, D. Großmann, W. Grünert and B. M. Reddy, *Appl. Catal., B*, 2014, **144**, 900–908.
- 29 J. He, G. K. Reddy, S. W. Thiel, P. G. Smirniotis and N. G. Pinto, *J. Phys. Chem. C*, 2011, **115**, 24300–24309.
- 30 W. D. Zhang, B. S. Liu, Y. P. Zhan and Y. L. Tian, *Ind. Eng. Chem. Res.*, 2009, **48**, 7498–7504.
- 31 G. Attard and C. Burnes in *Surfaces, Spectroscopic Techniques for Probing Solid Surfaces*, Oxford University Press, Oxford, 1998.
- 32 C. Suzuki, J. Kawai, M. Takahashi, A.-M. Vlaicu, H. Adachi and T. Mukoyama, *Chem. Phys.*, 2000, **253**, 27–40.
- 33 B. Mallesham, P. Sudarsanam and B. M. Reddy, *Catal. Sci. Technol.*, 2014, **4**, 803–813.
- 34 B. Mallesham, P. Sudarsanam, G. Raju and B. M. Reddy, *Green Chem.*, 2013, **15**, 478–489.
- 35 K. A. Nolin, R. W. Ahn and F. D. Toste, *J. Am. Chem. Soc.*, 2005, **127**, 12462–12463.
- 36 S. M. Landge, V. Atanassova, M. Thimmaiah and B. Török, *Tetrahedron Lett.*, 2007, **48**, 5161–5164.
- 37 S. Mallick, S. Rana and K. Parida, *Ind. Eng. Chem. Res.*, 2012, **51**, 7859–7866.
- 38 K. N. Tayade and M. Mishra, *J. Mol. Catal. A: Chem.*, 2014, **382**, 114–125.